Supplemental material JCB

Rocha et al., http://www.jcb.org/cgi/content/full/jcb.200811005/DC1

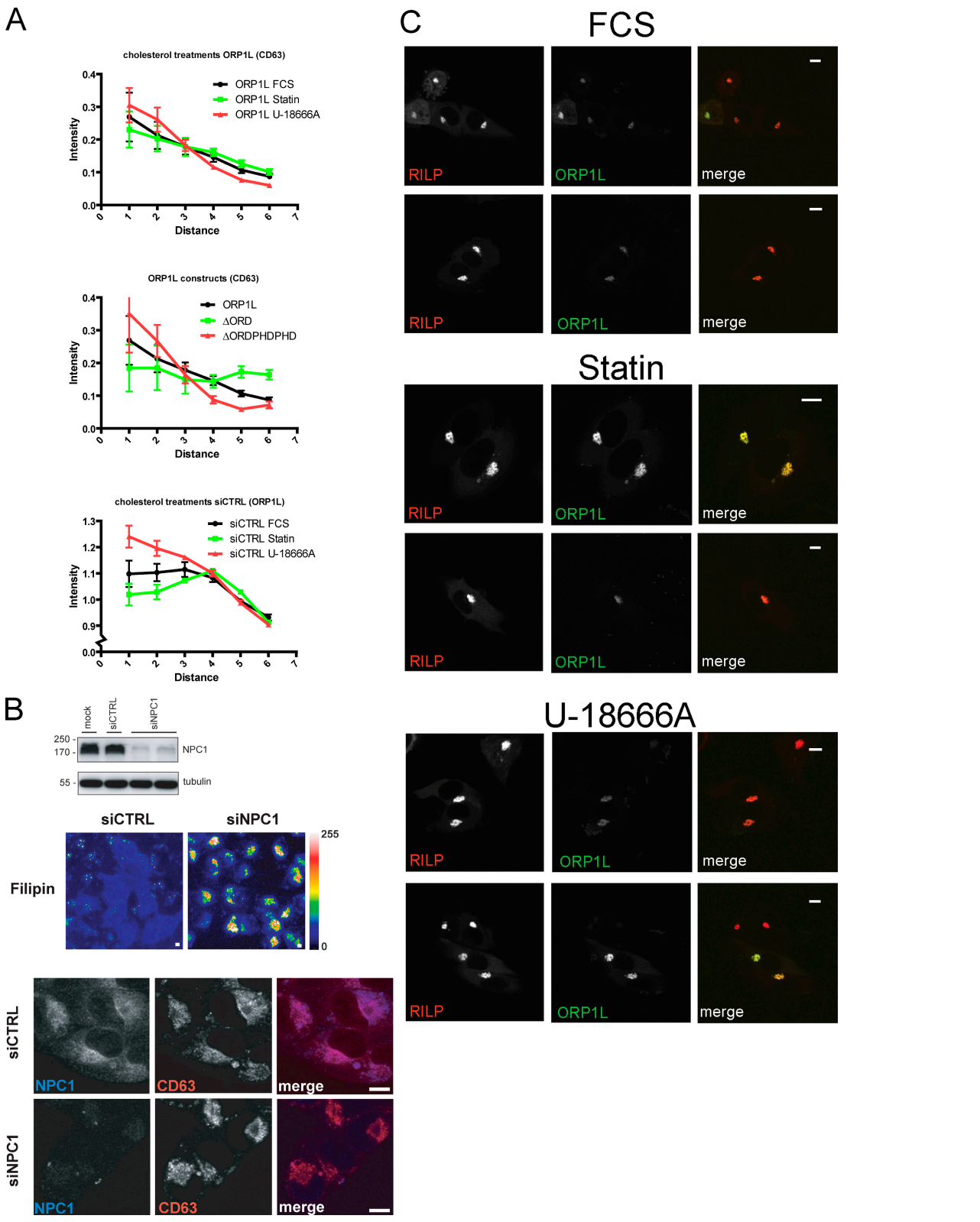

Figure S1. **Cholesterol, NPC1, the ORD, and vesicle distribution.** (A) LE distribution under expression of ORP1L and mutants or cellular cholesterol content modifications. (top) Cells were transfected with ORP1L and treated with U-18666A to enhance cellular cholesterol content (red) or with statin and delipidated FCS to decrease cellular cholesterol content (green) or not treated (black). Endogenous CD63 was stained with anti-CD63 (NKI-C3), and the radial distribution of the fluorescence was measured in six fractions with CellProfiler, in which fraction 1 starts in the center of gravity of the CD63 stain and subsequent fractions are progressively closer to the edge of the cell. (middle) Cells were transfected with ORP1L (black), ΔORD (green), and ΔORDPHDPHD (red). The distribution of the endogenous CD63 molecule was measured as described above. Vesicles cluster when the cholesterol content of cells is increased or when ΔORDPHDPHD is expressed. Scattering is observed when the cholesterol content of cells is decreased or when ΔORD is expressed. Mean and SEM values of >20 cells per condition are shown. The slopes of the curves were determined, and the dependence of vesicle distribution (based on mean intensity per fraction) on cholesterol content was tested (Jonckheere-Terpstra test) from enhanced (U-18666A) to control (FCS) to decreased cholesterol (statin) content ($P = 0.000257$2). In the case of the different ORP1L constructs (Fig. 2), vesicle distribution was tested from ΔORDPHDPHD (high cholesterol mimic) to ORP1L to ΔORD (low cholesterol mimic; $P = 5.122 \times 10^{5}$). (bottom) siRNA control (siCTRL)–transfected cells were treated with U-18666A to enhance cellular cholesterol content (red) or with statin and delipidated FCS to decrease cellular cholesterol content (green) or not treated (black). Endogenous ORP1L was stained with a rabbit polyclonal antibody. The radial distribution of the fluorescence was measured in six fractions with CellProfiler, in which fraction 1 starts in the center of gravity of the ORP1L stain, and subsequent fractions are progressively closer to the edge of the cell. The slopes of the curves were determined, and the dependence of vesicle distribution (based on mean intensity per fraction) on cholesterol content was tested (Jonckheere-Terpstra test) from enhanced (U-18666A) to control (FCS) to decreased cholesterol (statin) content ($P = 7.76 \times 10^{6}$). (B) LE vesicle distribution and cholesterol levels in NPC1-silenced cells and siRNA-mediated silencing of NPC1 and intracellular cholesterol. (top) MelJuSo cells were mock transfected or transfected with a control siRNA or siRNA for NPC1. After 72 h, cell lysates were separated by SDS-PAGE and Western blotting, and filters were probed with anti-NPC1 antibodies or tubulin antibodies as a loading control. The positions of the molecular mass standards are indicated in kilodaltons. (middle) MelJuSo cells were transfected with control (siCTRL) or NPC1 siRNA (siNPC1) for 72 h before fixation and staining with filipin. Images were made under identical settings, and a color LUT is applied to illustrate differences in intensities. $n > 200$ for each condition. (bottom) Effect of silencing NPC1 on LE positioning. MelJuSo cells were transfected with control of NPC1 siRNA before fixations and staining for NPC1 and the LE marker CD63, as indicated. $n > 100$. (C) RILP and ORLP1L binding under different cholesterol levels. MelJuSo cells were transfected with GFP-RILP and mRFP-ORP1L and exposed to control (FCS) or cholesterol-enhancing (U-18666A) or -decreasing (statin) conditions before fixation and analysis by CLSM. Representative images are shown. $n > 100$. No effect of cholesterol manipulation on GFP-RILP or mRFP-ORP1L binding to LEs is observed. Bars, 10 μm.

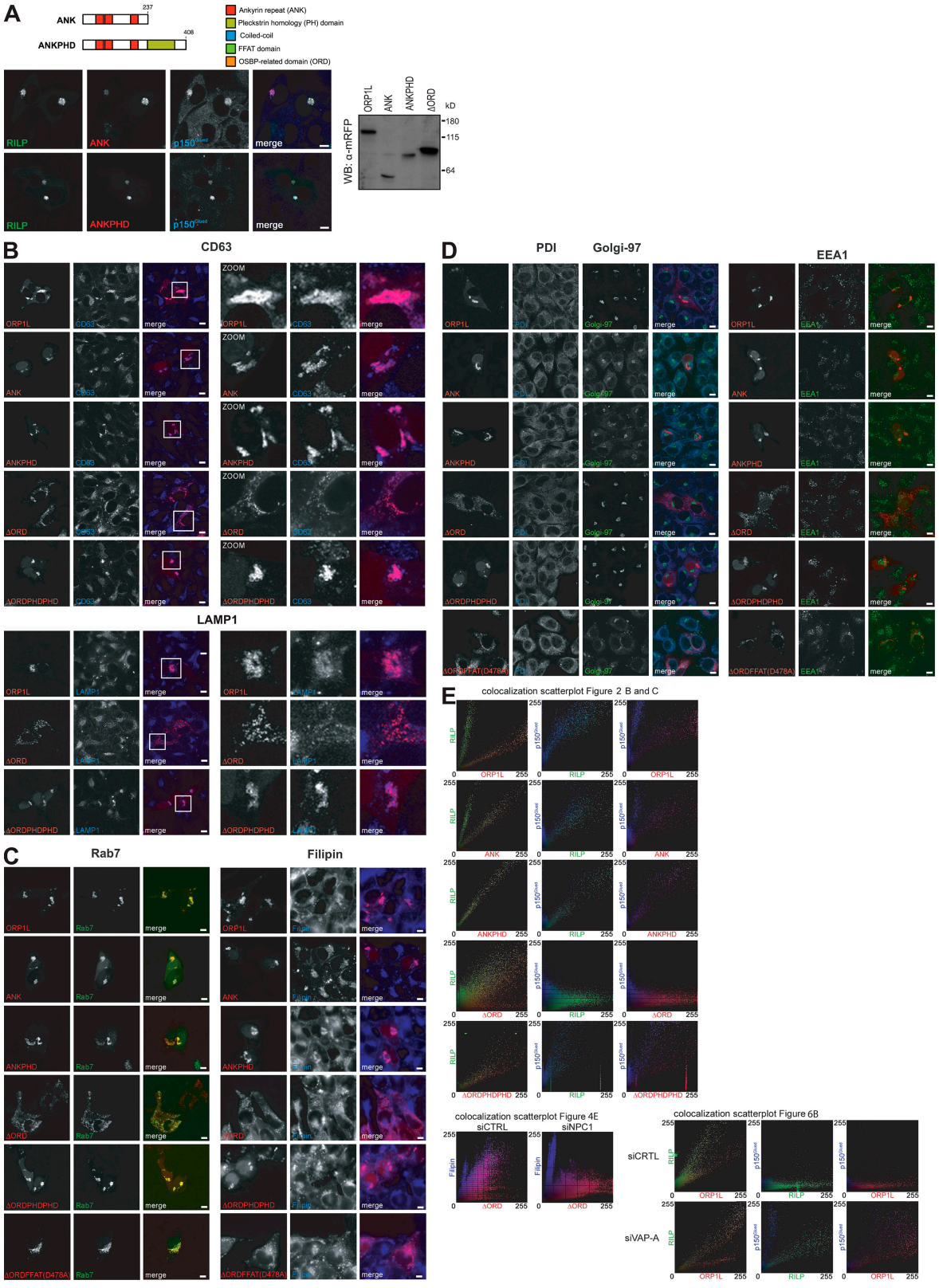

Figure S2. **Colocalization experiments of RILP and ORP1L variants with compartment markers and dynein motor subunits.** (A) ANK and ANKPHD enable recruitment of p150^{Glued} to the Rab7–RILP receptor. (top) ANK and ANKPHD domain structure and constructs. Numbers indicate amino acid residue positions. Both constructs were N-terminally tagged with mRFP. (bottom) Effect of ANK and ANKPHD chimeric constructs on RILP-mediated p150^{Glued} recruitment. (left) MelJuSo cells were transfected with GFP-RILP and mRFP-ORP1L constructs. Cells were fixed and stained with anti-p150^{Glued} antibodies before confocal microscopy. $n > 200$ for each condition. (right) MelJuSo cells were transfected with the indicated mRFP-ORP1L, -ANK, -ANKPHD, and -ΔORD constructs, and whole cell lysates were analyzed by SDS-PAGE and Western blotting with anti-mRFP antibodies (WB: α-mRFP). Positions of the molecular mass standards are indicated. WB, Western blot. (B) ORP1L and variants label CD63- and LAMP1-positive LEs. MelJuSo cells were transfected with various mRFP-

tagged ORP1L variants, as indicated. Cells were fixed and stained for CD63 or LAMP1. The right panel shows a zoom-in of the region where the vesicles locate. *n* > 100. (C) ORP1L and variants label Rab7- and cholesterol-positive vesicles. MelJuSo cells were transfected with various mRFP-tagged ORP1L variants, as indicated. Cells were fixed and stained for Rab7 or for cholesterol by filipin. *n* > 80. (D) ORP1L and variants do not label the ER, Golgi, or early endosomes. MelJuSo cells were transfected with various mRFP-tagged ORP1L variants, as indicated. Cells were stained and labeled for the ER marker protein disulfide-isomerase (PDI), the Golgi marker Golgi-97, or the early endosomal marker EEA1 (right). *n* > 100 for each panel. (E) 2D pixel analyses for colocalization of markers. The confocal microscopy images shown in Figs. 2 (B and C), 4 E, and 6 B were analyzed pixel by pixel for colocalization (intensity correlation analysis) of the markers indicated using ImageJ software (National Institutes of Health) with the WCIF plug-ins (http://www.uhnresearch.ca/facilities/wcif/imagej/). Proteins analyzed are shown along the x and y axes of the scatter plot in the color of analysis. Colocalization is indicated by a correlation in the x–y axis. Bars, 10 µm.

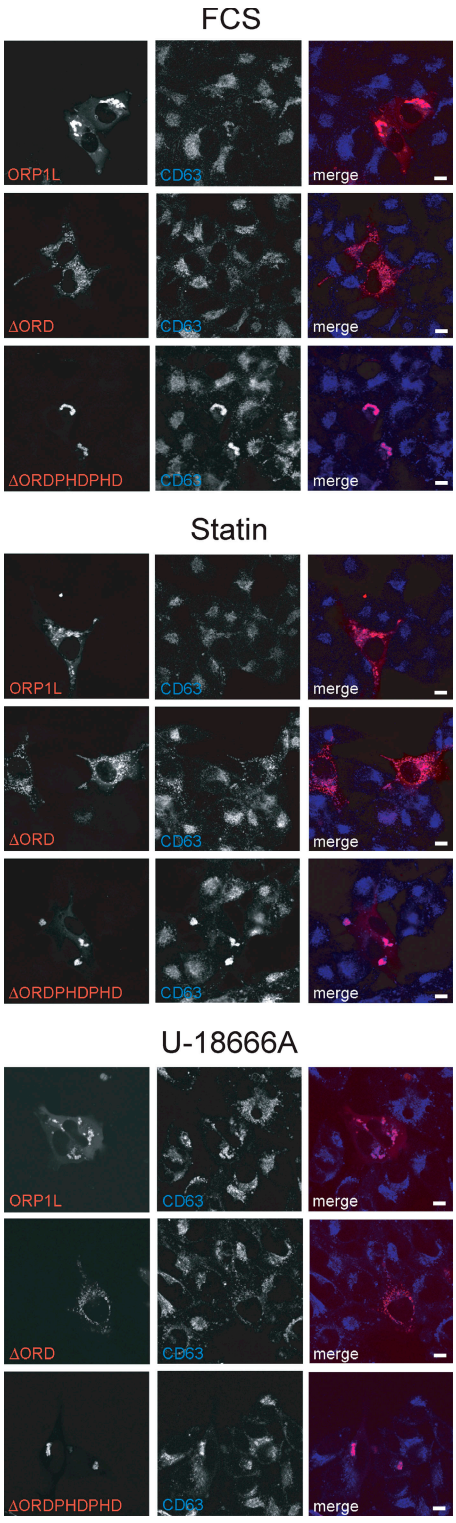

Figure S3. **Chemical manipulation of cholesterol levels and location of ORP1L variants on LEs.** MelJuSo cells were transfected with various mRFP-labeled ORP1L variants, as indicated, before intracellular cholesterol levels were decreased (statin) or increased (U-18666A). Cells were fixed and stained for the LE marker CD63, as indicated. $n > 50$. Bars, 10 µm.

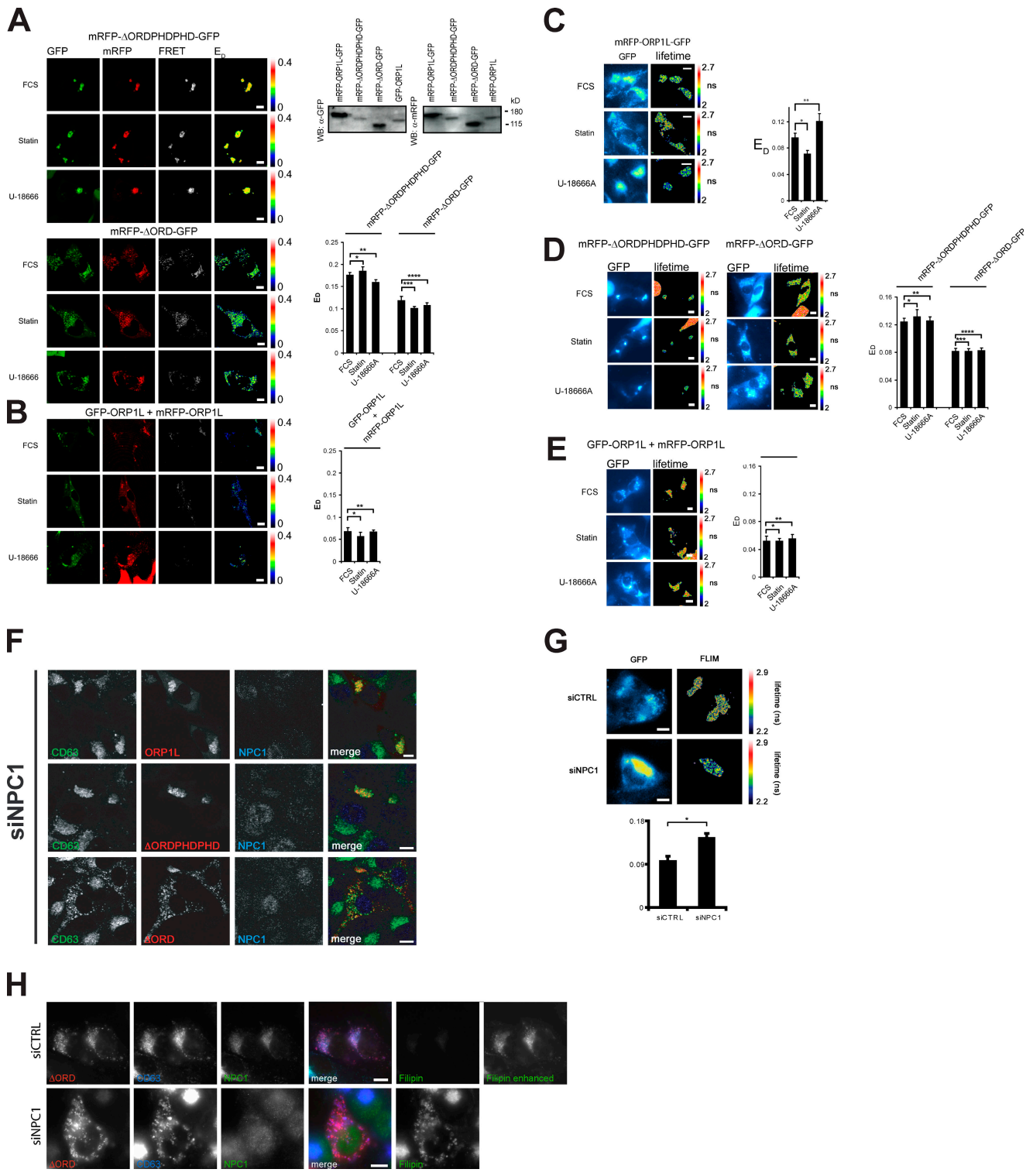

Figure S4. **Control-sensitized emission FRET and FLIM experiments, the effect of NPC1 silencing on ORP1L conformation, and vesicle distribution of ORP1L mutants.** (A) Sensitized emission confocal FRET for ORP1L variants and cholesterol level manipulations. MelJuSo cells were transfected with GFP-ΔORDPHD-PHD-mRFP or GFP-ΔORD-mRFP, and sensitized emission was determined under control conditions (FCS) or conditions of cholesterol depletion (statin) or accumulation (U-18666A). Cells were co-cultured with control cells expressing GFP or mRFP only, which were used to control for bleed through and indirect excitation (not depicted). (left) For the different constructs (as indicated), the GFP channel (after excitation with 488-nm light), the mRFP signal (after excitation with 568-nm laser light), FRET (after correction for bleed through and indirect excitation), and donor FRET efficiency (E_D) are shown. A color LUT directly reveals differences in donor FRET efficiency. (top right) The constructs tested in A–E and G were expressed, separated by SDS-PAGE and Western blotting, and probed with antibodies against GFP or mRFP, as indicated. The molecular mass standards are indicated. WB, Western blot. (bottom right) Donor FRET efficiency E_D plotted from eight measurements per condition. Mean ± SEM is shown (*, P = 0.33; **, P = 0.11; ***, P = 0.10; ****, P = 0.29). (B) Sensitized emission confocal FRET to test clustering GFP-ORP1L and mRFP-ORP1L under different conditions of cholesterol manipulation. MelJuSo cells were transfected with the two constructs GFP-ORP1L and mRFP-ORP1L and co-cultured with control cells expressing GFP or mRFP only. (left) Two control cells expressing

mRFP only are shown in the bottom panel. Cells were cultured under the various conditions of cholesterol manipulation before GFP, corrected mRFP, FRET, and donor FRET efficiency were measured, as described in A. (right) Quantification of donor FRET efficiency E_D calculated from nine measurements per condition. Mean ± SEM is shown (*, P = 0.39; **, P = 0.98). (C and D) FLIM to detect conformational changes in ORP1L variants in response to cholesterol level manipulations. MelJuSo cells were transfected with GFP-ORP1L-mRFP (C) or GFP-ΔORDPHDPHD-mRFP or GFP-ΔORD-mRFP (D), and GFP fluorescence lifetime was determined under control conditions (FCS) or conditions of cholesterol depletion (statin) or accumulation (U-18666A). (left) Cells were co-cultured with control cells expressing GFP only as an internal control for GFP lifetime not involved in a FRET pair. FLIM was measured by wide-field microscopy. The GFP panel shows the GFP signal, and the FLIM panel shows the fluorescence lifetime in nanoseconds, which is visualized using a color LUT. (right) Quantification of donor FRET efficiency E_D for the FRET constructs calculated from 20 measurements per condition. Mean ± SEM is shown (for C: *, P = 4.9×10^{-7}; and **, P = 9.5×10^{-12}; for D: *, P = 0.28; **, P = 0.74; ***, P = 0.98; and ****, P = 0.83). (E) FLIM measurements to test clustering of GFP-ORP1L and mRFP-ORP1L under different conditions of cholesterol manipulation. MelJuSo cells were transfected with the two constructs, GFP-ORP1L and mRFP-ORP1L, and co-cultured with control cells expressing GFP only before exposure to the conditions of cholesterol manipulation, as in C and D. (left) Wide-field image of GFP fluorescence and lifetime detection, which is shown in false colors for lifetime differences, as shown by a color LUT. (right) Calculated donor FRET efficiency E_D under the different conditions of cholesterol manipulation from 20 measurements. Mean ± SEM is shown (*, P = 0.94; **, P = 0.63). (F) Silencing NPC1 and location of ORP1L variants on CD63-containing endosomes. MelJuSo cells were transfected with siRNA for NPC1 and 48 h later with the various mRFP-labeled ORP1L constructs, as indicated. After another 24 h, cells were fixed and stained for the LE marker CD63 and NPC1 to control for actual silencing. $n > 100$. (G) ORP1L conformation in NPC1-deficient cells as detected by FLIM. mRFP-ORP1L-GFP–expressing MelJuSo cells were transfected with control (siCTRL) or NPC1 (siNPC1) siRNAs. (top) GFP fluorescence detected the distribution of the ORP1L-containing vesicles by wide-field microscopy. GFP lifetime was detected by FLIM. The lifetime was determined (in nanoseconds) and plotted in a false color LUT. (bottom) donor FRET efficiencies (E_D) as calculated from the FLIM data. The mean and SD from 75 cells analyzed in three independent experiments are shown (*, P = 3.1×10^{-16}). (H) LE scattering in NPC1-deficient cells. MelJuSo cells were transfected with control siRNA or siRNA for NPC1 and 48 h later with mRFP-ΔORD. 24 h later, cells were fixed and stained for the LE marker CD63, NPC1 (as control), and filipin to detect cholesterol. Microscopy images were made under identical settings. An additional image for filipin made after long exposure is shown (filipin enhanced) to show that control cells also contain cholesterol. $n > 50$. Bars, 10 μm.

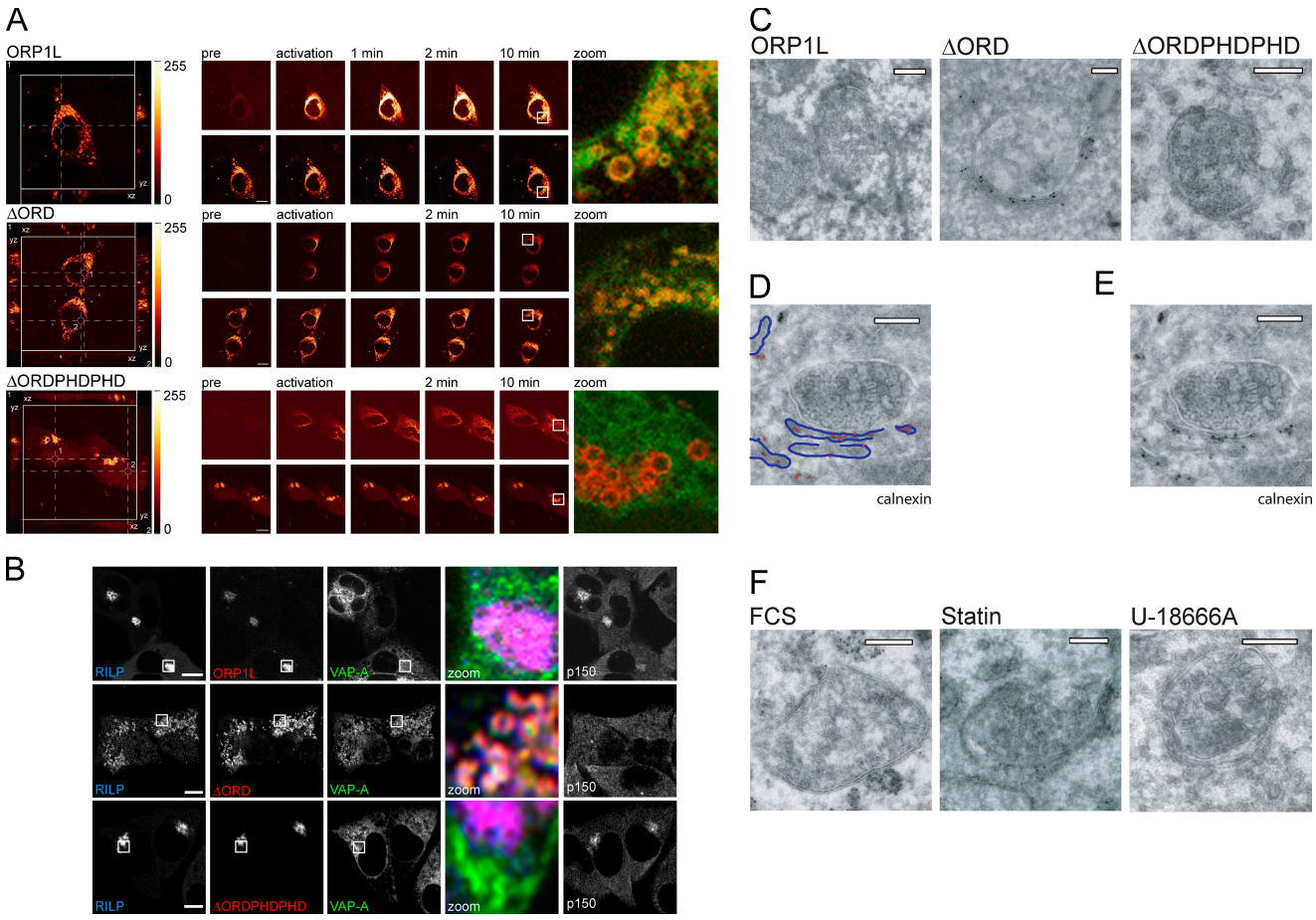

Figure S5. **ORP1L-mediated recruitment VAP-A from the ER and the release of p150^{Glued} from RILP.** (A) ORP1L recruits VAP-A from the ER. PA-GFP–tagged VAP-A in mRFP-ΔORDPHDPHD, -ΔORD, or -ORP1L–expressing MelJuSo cells was photoactivated with a 405-nm light to follow transport of ER-located PA-GFP–VAP-A to LEs by time-lapse microscopy. First, a z stack of cells was made to identify a location for selective photoactivation of the ER pool of VAP-A. The left shows an x–y, x–z, and y–z projection through the site of photoactivation (the 405-nm laser spot position is shown as a circle). Cells were followed by time-lapse confocal microscopy, and various snapshots of the mRFP and GFP channels before and after photoactivation of PA-GFP–VAP-A are shown. Images are presented in glow-over/under mode to represent different fluorescent intensities. The right panel shows a magnification of LEs (indicated by the boxed area) and a merge of the mRFP and GFP channel. $n > 10$ for each condition. See Videos 1–3. (B) VAP-A recruitment by ΔORD and release of p150^{Glued} from RILP. MelJuSo cells were transfected with GFP-RILP, mRFP-ORP1L constructs (as indicated), and HA-tagged VAP-A before fixation and staining with anti-HA and anti-p150^{Glued} antibodies before four-color confocal microscopy. The boxed area in the images indicates the zoomed-in region shown in overlay colors as the fourth panel. The right panel shows p150^{Glued}. ΔORD recruits VAP-A and excludes p150^{Glued} from RILP resulting in scattered vesicles. (C) Electron micrographs of multivesicular bodies in MelJuSo cells expressing HA-VAP and different variants of GFP-ORP1L, as indicated. Cells were fixed, and cryosections were stained with anti-HA antibodies detected with 15-nm gold particles. These images correspond to Fig. 8 A. (D) Electron micrographs of multivesicular bodies in MelJuSo cells expressing GFP-ΔORD. Cryosections were labeled with anticalnexin antibodies detected by 15-nm gold particles. The gold particles are highlighted by red dots, and the ER membrane is indicated by blue lines. (E) Original electron micrograph from multivesicular bodies in MelJuSo cells expressing GFP-ΔORD. Cryosections were labeled with anticalnexin antibodies detected by 15-nm gold particles. This image corresponds to D. (F) Electron micrographs of multivesicular bodies in HA-VAP– and GFP-ORP1L–expressing MelJuSo cells exposed to different cholesterol-manipulating conditions, as indicated. Cells were fixed and stained with anti-HA antibodies marked by 15-nm gold particles. These images correspond to Fig. 8 C. Bars: (A and B) 10 µm; (C–F) 200 nm.

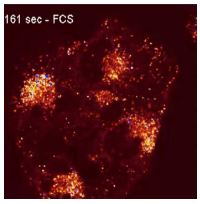

Video 1. **Motility of LEs in untreated cells.** LysoTracker red was used to label LEs in MelJuSo cells. Vesicle movement is visualized as a ratiometric glow LUT. Cells were imaged using a Leica SP2 system equipped with a heated chamber (37°C with 5% CO_2). Frames were taken every 1.6 s. The video is shown at 10 frames/s with 100 total frames.

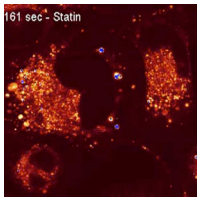

Video 2. **Motility of LEs in cholesterol-depleted cells.** LysoTracker red was used to label LEs in MelJuSo cells, which were cultured and imaged in cholesterol-depleted medium containing statins overnight (as in Fig. 1, A and B). Vesicle movement is visualized as a ratiometric glow LUT. Cells were imaged using a Leica SP2 system equipped with a heated chamber (37°C with 5% CO_2). Frames were taken every 1.6 s. The video is shown at 10 frames/s with 100 total frames.

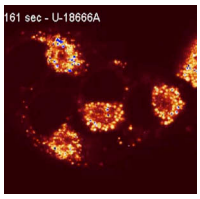

Video 3. **Motility of LEs in cholesterol-enriched cells.** LysoTracker red was used to label LEs in MelJuSo cells, which were cultured and imaged in medium containing U-18666A (as in Fig. 1, A and B). Vesicle movement is visualized as a ratiometric glow LUT. Cells were imaged using a Leica SP2 system equipped with a heated chamber (37°C with 5% CO_2). Frames were taken every 1.6 s. The video is shown at 10 frames/s with 100 total frames.

Video 4. **Repositioning of LEs in cells expressing the ORP1L-ΔORD mutant.** MelJuSo cells stably expressing CD63-GFP (green) to label LEs were microinjected with vectors encoding mRFP-ΔORD (red), H2B (histone-2B)-GFP (green; nuclear) as an expression control, and 70-kD Texas red dextran as an injection marker in the presence of cycloheximide. The cycloheximide block was washed away 2 h after microinjection. Cells were imaged using a Leica SP2 system equipped with a heated chamber (37°C with 5% CO_2). Frames were taken every 10 min. The video is shown at 5 frames/s with 30 total frames.

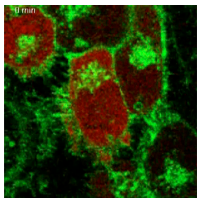

Video 5. **Repositioning of LEs in cells expressing the ORP1L-ΔORDPHDPHD mutant.** MelJuSo cells stably expressing CD63-GFP (green) to label LEs were microinjected with vectors encoding mRFP-ΔORDPHDPHD (red), H2B (histone-2B)-GFP (green; nuclear) as an expression control, and 70-kD Texas red dextran as an injection marker in the presence of cycloheximide. The cycloheximide block was washed away 2 h after microinjection, immediately before imaging. Cells were imaged using a Leica SP2 system equipped with a heated chamber (37°C with 5% CO_2). Frames were taken every 10 min. The video is shown at 5 frames/s with 30 total frames.

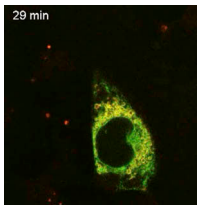

Video 6. **VAP-A diffusion in cells expressing ORP1L.** MelJuSo cells were transiently transfected with expression vectors for PA-GFP–VAP-A (green) and mRFP-ORP1L (red). PA-GFP–VAP-A was activated by a 405-nm laser at a site where the ER is present but LEs are not. To exclude that the 405-nm laser beam would hit LEs, a z stack was made to locate ER pools of VAP-A away from the mRFP-labeled LEs. Cells were imaged using a Leica AOBS system equipped with a 37°C chamber culture hood with 5% CO_2. Frames were taken every 1 min. The video is shown at 3 frames/s with 30 total frames. The still images are presented in Fig. S5 A.

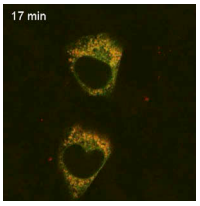

Video 7. **VAP-A diffusion in cells expressing the ORP1L-ΔORD mutant.** MelJuSo cells were transiently transfected with expression vectors for PA-GFP–VAP-A (green) and mRFP-ΔORD (red). PA-GFP–VAP-A was activated by a 405-nm laser at a site where the ER is present but LEs are not. To exclude that the 405-nm laser beam would hit LEs, a z stack was made to locate ER pools of VAP-A away from the mRFP-labeled LEs. Cells were imaged using a Leica AOBS system equipped with a 37°C chamber culture hood with 5% CO_2. Frames were taken every 1 min. The video is shown at 3 frames/s with 30 total frames. The still images are presented in Fig. S5 A.

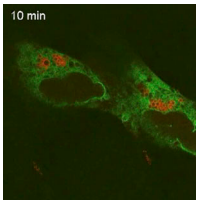

Video 8. **VAP-A diffusion in cells expressing the ORP1L-ΔORDPHDPHD mutant.** MelJuSo cells were transiently transfected with expression vectors for PA-GFP–VAP-A (green) and mRFP-ΔORDPHDPHD (red). PA-GFP–VAP-A was activated by a 405-nm laser at a site where the ER is present but LEs are not. To exclude that the 405-nm laser beam would hit LEs, a z stack was made to locate ER pools of VAP-A away from the mRFP-labeled LEs. Cells were imaged using a Leica AOBS system equipped with a 37°C chamber culture hood with 5% CO_2. Frames were taken every 1 min. The video is shown at 3 frames/s with 30 total frames. The still images are presented in Fig. S5 A.